doi:10.20944/preprints202007.0056.v1

Article

A theoretical and experimental study on the potential luminescent and biological activities of diaminodicyanoquinodimethane derivatives.

Edison Rafael Jiménez [1], Manuel Caetano[1], Nelson Santiago[2], F. Javier Torres[3], Thibault Terencio[1,] * and Hortensia Rodríguez [1,]*

[1] School of Chemical Sciences and Engineering, Yachay Tech University. Hda. San José s/n y Proyecto Yachay, 100119, Urcuquí, Ecuador; edison.jimenezg@yachaytech.edu.ec (E.R.J.); mcaetano@yachaytech.edu.ec (M.C.)
[2] School of Biological Sciences and Engineering, Yachay Tech University. Hda. San José s/n y Proyecto Yachay, 100119, Urcuquí, Ecuador; nvispo@yachaytech.edu.ec (N.S.)
[3] Instituto de Simulación Computacional (ISC-USFQ), Universidad San Francisco de Quito, Diego de Robles y Vía Interoceánica, Quito 17-1200-841, Ecuador.: jtorres@usfq.edu.ec (F.J.T.)
* Correspondence:hmrodriguez@yachaytech.edu.ec ; Tel.: + 593 6 2 999 500 ext. 2622 (H.R.)
tterencio@yachaytech.edu.ec (T.T.)

Abstract: Since the discovery of the aggregation-induced emission effect in 2001, diaminodicyanoquinone derivatives (DADQs) have presented interesting fluorescence properties, allowing them to be considered fluorescent dyes capable of showing quantum yields above 90%. Besides, the diaminodiacyanoquinone core represents a versatile building block propense either to modification or integration into different systems to obtain and provide them unique photophysical features. Herein, we carried out a theoretical study on the fluorescence properties of three different diaminodicyanoquinodimethane systems. Therefore, time-dependent density functional theory (TD-DFT) was used to obtain the values associated with the dipole moments, oscillator strengths, and the conformational energies between the ground and the first excited states of each molecule. The results suggest that only two of the three studied systems possess significant luminescent properties. In a further stage, the theoretical insights were confirmed by means of experimental measurements, which not only retrieved the luminescence of the DADQs, but also suggest a preliminary and promising antibacterial activity of these systems.

Keywords: Aggregation-induced emission; quinones; fluorescence; TD-DFT; quantum yield

1. Introduction

Within the luminescence context, luminophores are species having the capacity of emitting light with apparent spontaneity. These systems are the basis of the development of luminescent materials, which in turn have potential applications in a number of new technologies. [1] Thus, a great deal of attention has been paid to thoroughly understand the properties of luminescent materials as well as the underlying light-emitting processes. Indeed, the work conducted on the discovery and development of green fluorescent proteins (GFP) was awarded with the Nobel Prize back in 2008. [2]

Although, luminophores should be, in principle, capable of emitting electromagnetic radiation independently of their physical state. Most of the practical applications require luminophores to be synthesized as solid-films, aggregates, or crystals.[3], [4] For example, solid-state organic light-emitting diodes (OLEDs) and organic field-effect transistors (OFETs)[1], [5] are considered essential components in optoelectronic or sensing applications for ecosystem monitoring and biomedical research.[6]–[8]

doi:10.20944/preprints202007.0056.v1

In these regards, it is important to point out that highly conjugated molecules are the most common way to obtain luminescence in organic molecules. Therefore, highly conjugated species and even more aromaticity are imperative characteristics when one wants to synthesize luminescent molecules. Additionally, it is important to mention that the vicinity of luminophores on condensed phases or at high concentration produces the so-called aggregation-caused quenching or simply ACQ. [9], [10] The latter effect represents an enormous limiting factor for the performance of luminescent materials, and it can be attributed to the removal of excited states caused by the strong π−π stacking interaction involving the aromatic groups of the luminophores. In order to overcome the aforementioned limitation Luo and co-workers proposed in 2001 a novel kind of organic-luminogenic materials, which upon aggregation, increases its radiative emission rather than decreasing it. [11] This pioneering study was followed by subsequent works where a series of silole derivatives, presenting the so-defined aggregation-induced emission (AIE), were reported. [4], [12] [REF] As stated in the latter, a thorough understanding of the underlying mechanism of the AIE effect is fundamental for the conversion of materials with poor luminescent potential into building blocks of high-tech optical innovations. [13]–[15]

During the last years, significant progress has been made in this matter, resulting in the synthesis of a great variety of AIE luminogens (AIEgens), capable of emitting at different wavelengths. This has not only brought new insights into the light-emission processes but has widen the possibilities for the development of new application. However, open questions are yet present in the field and research efforts are still needed. In these regards, computational approaches represent interesting tools for the study of the fluorescence capabilities of different already designed systems. In particular, these approaches allow a better understanding of the AIEgens luminescence mechanism to be achieved, making possible, at the same time, to assess the molecular characteristics (i.e., geometries, conformational changes, and their oscillator and dipole moments) controlling the luminescent potential of a given system.

The aim of the present work is to demonstrate that theoretical calculations provide truthful information on how different substitutions for benzene functionalized DADQs can enhance or quench the AIE effect. Once the theoretical predictions were verified, an additional preliminary antibacterial activity of the DADQs derivatives was carried out, showing its potential as growth inhibitors for *Escherichia coli DH5* strains. Additionally, the influence that exert different changes in the structural compositions of the synthesized molecules can alter their inhibitory capacity is studied.

2. Results

2.1. Theoretical investigation

At first, a structural computational research of three molecules, 2-(4-(imidazolidin-2-yl)phenyl)malonitrile **1**; 2-(4-(1-(4-nitrophenyl)imidazolidin-2-yl)phenyl)malononitrile **2** and 2-(4-(1-(2-nitrophenyl)imidazolidin-2-yl)phenyl)malononitrile **3** **(Figure 1)** were analyzed to obtain insights into the possible reasons for fluorescence quenching or enhancement produced in these molecules. We performed time-dependent density functional theory calculations (TD-DFT) at the CAM-B3LYP level using acetonitrile as the implicit solvent model.

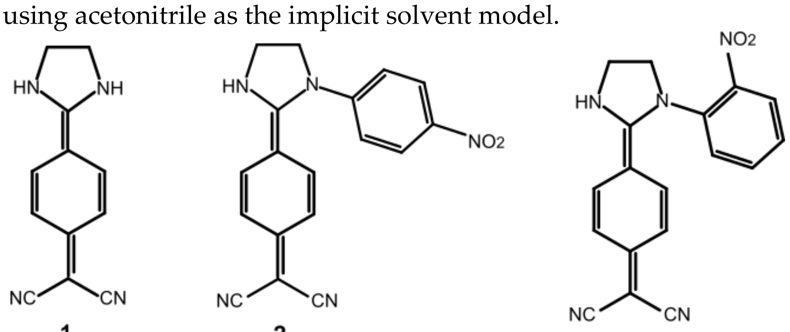

1 **2** **3**

Figure 1. Molecular structure of the target molecules.

For a molecule to have high quantum yields (QY), the difference between its ground state equilibrium geometry and its excited counterpart must be minimal. Notably, the ground (S_0) and excited (S_1) state structures of compounds **1** and **2** were found to be very similar, whereas for compound **3** the changes were much more noticeable.**(Figure 2)** Furthermore, compound **3** in its excited state exhibits a curvature in the quinone moiety bearing two cyano groups (**Figure 2.f.** red structure).

Planarity is always a reflect of electron delocalization between different atoms: in this case, this loss of planarity reflects a loss of aromaticity in the molecule. In order to quantify this loss of aromaticity in compound **3**, we computed the Nucleus Independent Chemical Shift (NICS) indexes to estimate the aromaticity of the quinone part. (**Table 1**). The indexes were computed both at the center of the quinone ring (NICS(0)) and at a distance of 1Å (NICS(1)) from the center to estimate the effect mainly produced by the pi system.

		NICS(0)$_{iso}$	**NICS(1)$_{iso}$**	**NICS(0)$_{zz}$**	**NICS(1)$_{zz}$**
	1	-4.0	-6.3	2.5	-15.8
S_0	**2**	-3.7	-6.0	3.8	-14.1
	3	-4.3	-6.8	2.0	-16.2
	1	-5.2	-7.4	-1.9	-19.3
S_1	**2**	-5.5	-7.6	-3.2	-18.5
	3	-5.7	-7.6	-3.1	-19.8

Table 1. NICS indexes of aromaticity of the quinone ring in the the compounds **1**,**2** and **3**. (0) specify at the center of the ring. (1) specify it is calculated at a distance of 1Å perpendicular to the plane of the quinone ring. Iso is based on the isotropic shielding while zz is the zz-component of the shielding.

Different types of NCIS indexes can be calculated, nevertheless, the out-of-plane NICSzz descriptor was shown to be one of the most reliable.[16] According to this descriptor, there is an increase of aromaticity upon excitation from S0 to S1 in all three compounds. This observation apparently contradicts the loss of aromaticity in compound **3** upon excitation while a curvature of the quinone ring is definitely observed in this molecule. NCIS indexes are a great tool to estimate aromaticity but are known to suffer from different shortcomings. In this particular case the structural change observed is totally non-local while NCIS indexes are evaluated at specific points. In fact, Through a close inspection of the indexes arises an interesting observation: there are increment of NICS(1)$_{zz}$ by 4.4 and 3.6 for compounds **2** and **3** respectively. While NCIS indexes cannot grasp this loss of aromaticity, it allows to conclude on a differential effect of excitation on compounds **2** and **3** regarding aromaticity.

Since the only difference between compounds **2** and **3** is the position of the nitro group (para and ortho respectively), the cause of the curvature encountered for the excited state of the compound **3** probably lies in the presence of the nitro group. Nevertheless, there is not only change in the position of the nitro group between **2** and **3**, but also in its orientation. In compound **2**, the nitro group is in the same plane as the cycle, whereas a dihedral angle of *ca.* 30° is found in compound **3**. The implications of this on the electronic structure is detailed in supplementary materials through the presentation of charge distribution.

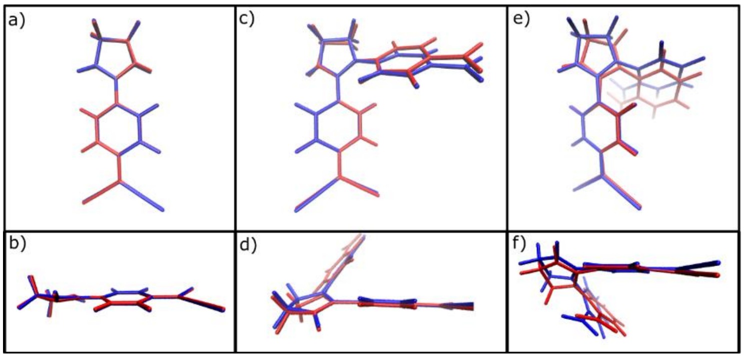

Figure 2. Comparison between the optimized ground state (blue) and excited state (red) structures. **a)** frontal view of molecule 1; **b)** lateral view of molecule 1; **c)** frontal view of molecule 2; **d)** lateral view of molecule 2; **e)** frontal view of molecule 3; **f)** lateral view of molecule 3.

Additionally, it is essential to check the oscillator strengths and dipole moments associated with each molecule. In these regards, the calculated oscillator strengths and dipole moments for each of the studied compounds would provide a good idea on which of them will present the AIE effect and which do not **(Table 2)**.

		1	**2**	**3**
Oscillator Strength	S_0	1,2520	0,7850	0,0030
	S_1	1,2889	1,0087	0,0005
Dipole moment (Debye)	S_0	29,3167	31,0528	30,5951
	S_1	27,1140	28,5555	31,0556

Table 2. Oscillator strength and dipole moments of compounds **1**, **2,** and **3** in the ground and excited state.

2.2. Experimental investigation

Additionally, to corroborate the theoretical results obtained, the synthesis and structural characterization of **1** and **2** were performed. Finally, biological activity tests were conducted on the synthesized molecules to obtain further insight into their possible future applications.

Compounds **1** and **2** were synthesized followed a previously reported procedure. [17] Initially, 7,7,8,8-Tetracyanoquinodimethane (TCNQ) was reacted with a sacrifice pyrrolidine to favor substitution in the geminal cyano group of TCNQ. This 7-pyrrolidino-7,8,8-tricyano quinomethane (PTCNQ) reacts with the respective amines to form compound **1** and **2** **(Figure 3)** with 70 and 50% yields, respectively. Characterization of compounds **1** and **2** were carried out by analytical and spectroscopic techniques (UV-VIS, FTIR and mass spectroscopy) allowed to corroborate the derivatives structures (See Supporting Information). The synthesis of **3** was not possible, probably, due to the robust stability present in one of the initial reagents.

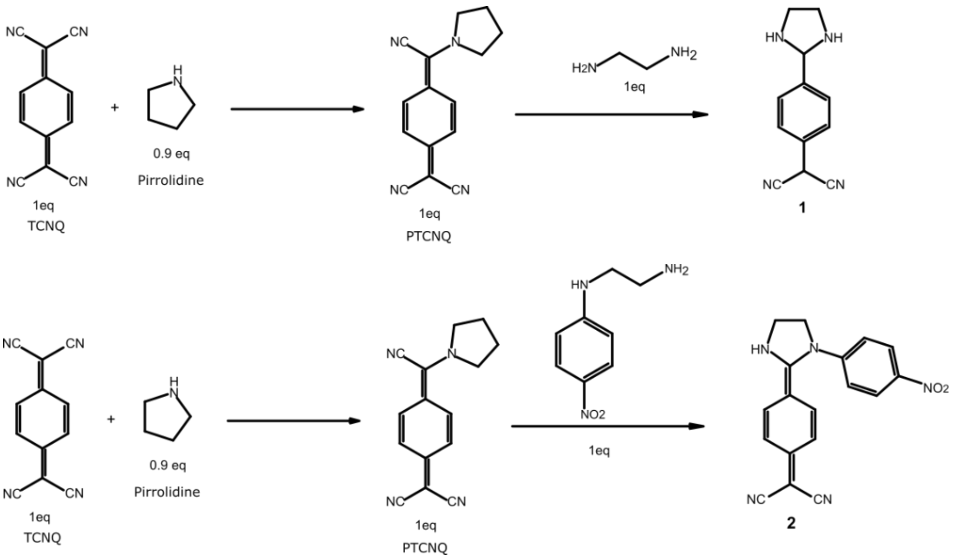

Figure 3. Synthetic route starting with the activation of TCNQ, to obtain molecules **1** and **2**.

Additionally, the emission spectra of **1** and **2** were recorded in all visible range and corrected for the blank (solvent) to perform proper emission intensity integration (**Figure 4)**. The relative quantum yield (QY) of **2** in dimethyl sulfoxide (DMSO) as the solvent system was calculated, obtaining a value of 15.64%. Accordingly, the QY of **1** in DMSO corresponds to 10.1%. [17]

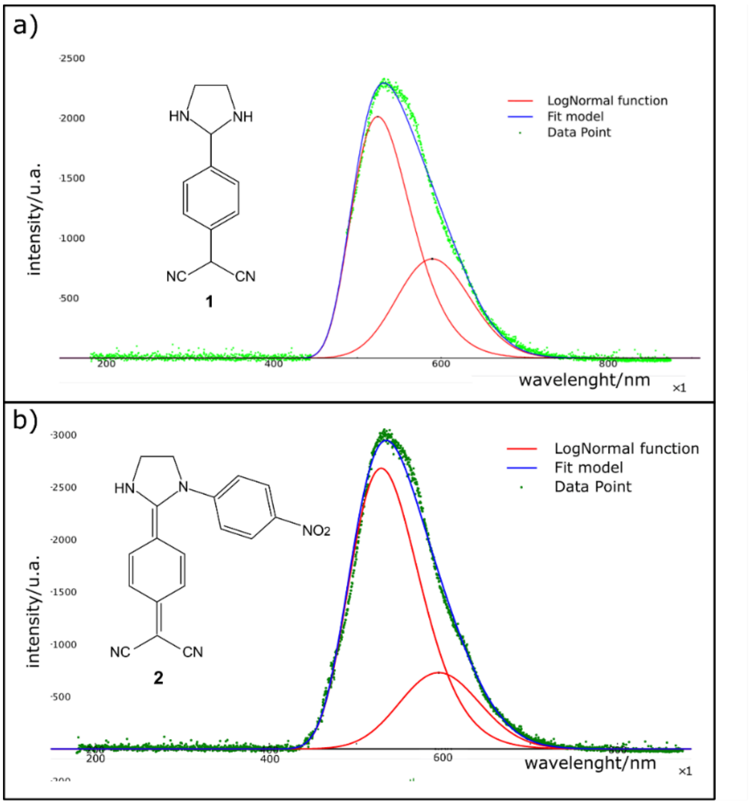

Figure 4. Recorded emission spectra in all the visible range. a) Emission spectra and its proper deconvolution of molecule **1**; b) Emission spectra and its proper deconvolution of molecule **2**.

2.3. Biological Investigation

The results obtained for the agar diffusion technique exhibited inhibition zones for all the tested molecules. Also, it is essential to remark that the solvent system by itself shows some sort of antibacterial activity, but it is not as important as the ones observed for the studied compounds.

doi:10.20944/preprints202007.0056.v1

Additionally, the antibacterial activity of the tested molecules is appreciable at concentrations of 1000 µg/ml and the 100 µg/ml, while for lower concentrations, the inhibition zones a barely perceptible and could be mostly because of the solvent system rather than the samples itself.

The results for the OD_{600} studies showed that all the compound presents antibacterial activity **(Figure 5).** Additionally, it has been demonstrated that *E. coli* cultures with an OD_{600} of 0.1 and incubated in a LB Broth present a concentration around 8 x 10^8 cells/ml.[18], [19]

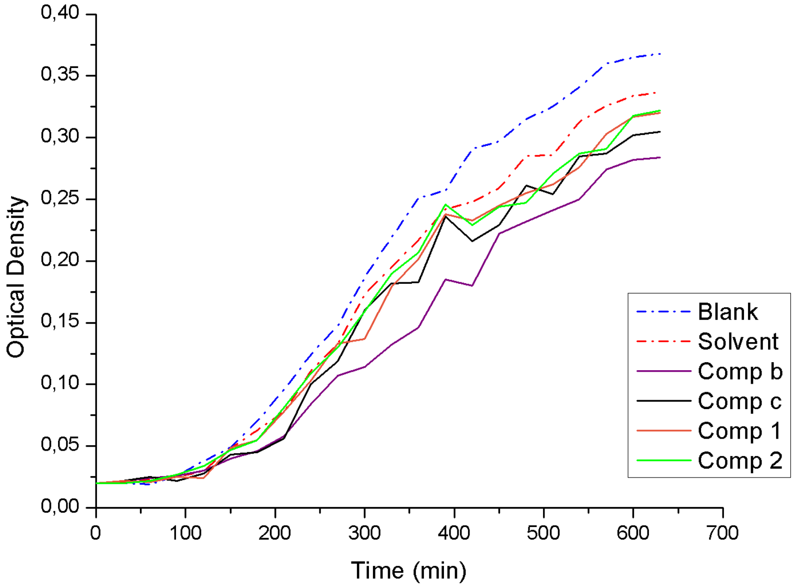

Figure 5. Growth curves for the OD600 tests performed to five different test tubes, blank (growth curve under standard conditions); Solvent (growth curve under the presence of the used solvent); PTCNQ (growth curve under the presence of PTCNQ)); Comp.1 (growth curve under the presence of compound **1**); Comp.2 (growth curve under the presence of compound **2**); Comp c (growth curve under the presence of compound N-(4-nitrophenyl)ethylenediamine)).

Therefore, the solvent by itself is capable of inhibiting the *E. coli* growth in values around 8,5% in comparison with the standard conditions of growth (Blank); henceforth, the other test tubes must take in account the solvent´s activity and will be directly compared with the inhibition capacity of the latter one. Consequently, compounds **1** and **2** showed a reduction of 4.7 and 4.4 %, respectively. Whereas, **c** reaches an inhibition capacity of 7.9% and **b** reaches the highest inhibition capacity, with a value of 14.3% **(Table 3).**

	OD_{600}	cells/ml	% cells growth	% of inhibition
Standard	0.1	8 x 10^8	-	-
Blank	0.365	2.92 x 10^9	100	0
Solvent	0.334	2.672 x 10^9	91.50684932	8.5
Comp b	0.282	2.256 x 10^9	77.26027397	14.3
Comp c	0.305	2.440 x 10^9	83.5616440	7.9
Comp 1	0.317	2.536 x 10^9	86.84931507	4.7
Comp 2	0.318	2.544 x 10^9	87.12328767	4.4

Table 3. Final OD600 values, the estimated number of cells per ml, and percentages of inhibition for each growth curve.

doi:10.20944/preprints202007.0056.v1

3. Discussion

Relative to the theoretical estimation of luminescence, the ground (S_0) and excited (S_1) states of compound **1** and **2** hardly differ from each other, fulfilling the condition of presenting a close similarity between the relaxed structures of the excited state and the ground state without IC or ISC influencing the photoexcitation process. Whereas for molecule **3** the geometrical differences are quite significant, indicating an absence or very low QY for this specie. Accordingly, for **1** there are oscillator strength values of 1.232 and 1.2889 for the ground and excited states respectively, and for **2** there are values of 0.785 and 1.0087 for the S_0 and the S_1 states respectively, indicating in both cases that the electronic transitions are quantum-mechanically allowed. However, for **3** there are oscillator strength values of less than 0.01, indicating that the transitions in this compound are restrained; therefore, any kind of fluorescence in **3** can be discarded. For the dipole moment, the presence of a donor-acceptor system in our molecules will produce an electron shift from the dicyanomethane to the amine groups upon photoexcitation. These electronic transitions give rise to a reduction of the dipole moment in the excited state of around 2.5 D for **1** and **2**. In contrast, the dipole moment for **3** increases in 1.5 D. This means that compounds **1** and **2** it is expected to observe that the fluorescence spectrum will present a negative solvatochromism (blue-shift) when the polarity of the solvent is increased, while for compound **3** it is expected a positive solvatochromism with an increase in solvents polarity. As expected, compounds **1** and **2** showed not only luminescent activities but also similar QY in the experimental tests, demonstrating the validity of the theoretical approach.

Related to the synthesis, **1** and **2** were obtained by similar procedures previously described with minor modifications (See Supporting Information). For preparation of **3,** there could be several reasons for the no reaction between N-(2-nitrophenyl)ethylenediamine and 7-pirrolidino-7,8,8-tricyanoquinodimethane. One possibility is the formation of an intramolecular six-member ring stabilized by a hydrogen bond of the type (N–H···O) between oxygen (O) in the nitro group and the hydrogen (H) of the secondary amine present in the molecule. Moreover, through geometrical optimizations it has been found that the six-member ring formation is a viable hypothesis due to the distance of 1.82Å and angle of 110° that correspond to the expected values for a hydrogen bond and a six-member ring. This will highly reduce the reactivity of N-(2-nitrophenyl)ethylenediamine avoiding the formation of **3** (See Supporting Information).

The relative measured quantum yields in DMSO correspond to 10.1% and 15.64% for **1** and **2**, respectively. Additionally, the different densities between the ground state and excited state illustrate a shift in electron density between the dicyanomethane moiety and the diamine changeable groups upon photoexcitation. These changes lead to a reduction in the dipole moments of the molecules in the excited state, producing a negative solvatochromic effect. These quantum yield measurements show that N-substitutions could exert essential changes in the quantum yield values of DADQ's systems without significantly modifying the positions of the emission and absorption peaks.

On the other hand, the biological activities tests showed that **b** reduces the bacteria growth by 14%, **c** with a 7.9%, while compound **1** and **2** reduce it in 4.7% and 4.4%, respectively. Taking into account the chemical structures for each of the studied compounds and their respect inhibition capacity, it is possible that the cyano, the primary and secondary amine groups played an essential role in the antibacterial capacity in each of the molecules. Finally, comparing the antibacterial activities of **1** and **2**, it seems that the presence of the nitro-benzene moiety does not contribute to biological activity. However, it is necessary to perform more investigations to obtain further insight into the possible conformational changes that could affect the antibacterial activity of the DADQs derivative.

It will be of great interest to perform more research on the AIE characteristics of **2**. It was recording the quantum yields with different conditions like changing the temperature, solvent's viscosity, level of aggregation, or different concentrations. Additionally, for further insight into the relationship between the antimicrobial activity and the molecular structure of each compound, it would be necessary to perform the same proves with TCNQ and with 7,7-dipyrrolidino-8,8-tricyanoquinodimethane to understand the role of cyano and pyrrolidine groups for the antimicrobial activity.

doi:10.20944/preprints202007.0056.v1

4. Materials and Methods

All geometry optimizations were initially performed using a force field approach with Avogadro[20] and later with the, Gaussian 16 (revision A.03) suit of programs. [21] The ground and excited state optimizations were carried out at the CAM-B3LYP/def2-TZVP level of density functional theory (DFT). [22], [23] Additionally, calculations with the implicit solvent model (SCRF) were incorporated with acetonitrile as the solvent medium. Acetonitrile was used because is not a protic solvent, that could not induce fluorescence quenching by hydrogen bonding or a too viscous solvent, that would enhances the fluorescence due to its viscosity. [24]

CAM-B3LYP was used for this type of calculations because it has shown a very accurate performance for excited states and species displaying a strong charge-transfer character. In all cases as specified in the methodology section, the absolute minima of each structure were proved by showing no negative (imaginary) frequencies in the frequency calculations.

Synthesis procedures of **1** and **2** were carried out followed a reported procedure for analogous compounds [17]. For individual reactions yield, structures and its characterizations see supporting information.

Quantum yield measurements (QY) were performed using the comparative method of Williams *et al.*[25] Hence, for this approach, **1** was used as the standard sample and **2** as the test sample. Both were diluted in DMSO at a concentration of 200 μg/ml and placed in scrupulously clean 1cm fluorescence cuvettes. The emission spectra of both reference and sample were recorded in full and corrected for the blank (solvent only) to perform proper emission intensity integration. The configuration used for data collection was a 180° excitation-fluorescence detection geometry, with a slight deflection of the optical fiber from the excitation source to avoid any interference signal from the source. Also, the absorption (optical density) of both samples was recorded under the same conditions as the emission spectrum. Finally, the relative quantum yield (QY) of the sample in the solvent used (DMSO) was calculated according to in equation (1)

$$\Phi_x = \Phi_{st} \frac{Int_x}{Int_{st}} \left(\frac{1-10^{A_{st}}}{1-10^{A_x}} \right) \frac{n_x^2}{n_{st}^2} \tag{1}$$

Antibacterial activity was tested for compounds **1**, **2**, PTCNQ and N-(4-nitrophenyl)ethylenediamine) the two latter referred to as **b** and **c**, respectively. In order to estimate the antibiotic efficacy of the synthesized molecules, two techniques were used: (i) the agar diffusion technique and (ii) the optical density (OD600) measurements.

Optical density measurements were performed on a Thermo-scientific Nanodrop UV-Vis spectrophotometer. Absorbance measurements were taken every 30 minutes at 600 nm wavelength and room temperature. Six different test tubes were prepared with 2.5 ml of Luria Bertani (LB) broth base, and one colony of *E. coli* (DH5-alpha) strains to obtain an initial OD_{600} of 0.02. For tube 1, nothing else was added, while for tube 2, it was additionally added 100 μL of the solvent system (5:5; water/DMSO). For tubes 3, 4, and 5, it was added 100 μL of 1mg/ml solutions of compounds PTCNQ, **1** and **2**, respectively.

5. Conclusions

Computational calculations provide geometry conformation, dipole moments, and oscillator strengths values that establish potential luminescent capacities for compounds **1** and **2**, and denies the possibility to have this activity in compound **3**.

Compounds **1** and **2** were successfully synthesized and characterized, while a similar procedure gave no result for the preparation of compound **3**. We proposed that the unattainability of product **3** was due to the formation of a highly stable specie in one of its initial reagents, supported by theoretical calculations. The experimentally obtained quantum yields for **1** and **2** of 10.1% and 15.6%, respectively, confirm the obtained results in the theoretical section of this research. This study particularly highlights the predictive theoretical calculations as a powerful tool in the context of AIE effect study.

The biological activity test of these molecules reveals an inhibition capacity to *E. coli* strains, which could be related to the presence of cyano groups in the molecular structure of the studied molecules. In summary, synthesized diaminodicyanoquinones (DADQ´s) are valuable customizable fluorescent systems with potential photophysical and bio-luminescent applications.

Supplementary Materials: Supplementary materials can be found at www.mdpi.com/xxx/s1.

Author Contributions: Investigation, Edison Rafael Jimenez, Manuel Caetano, Nelson Santiago, F. Javier Torres, Thibault Terencio and Hortensia Rodriguez; Methodology, Edison Rafael Jimenez, Thibault Terencio and Hortensia Rodriguez; Supervision, Thibault Terencio and Hortensia Rodriguez; Writing – original draft, Edison Rafael Jimenez; Writing – review & editing, Thibault Terencio and Hortensia Rodriguez.

Funding: This research received no external funding. This study was funded by Yachay Tech internal Project ''Aggregation-induced emission Effect in Diaminodicyanoquinodimethanes derivatives''.

Acknowledgments: The authors thanks Mass spectroscopy core facility of School of Chemical Sciences and Engineering, Yachay Tech (Juan Pablo Saucedo, PhD and Ruth Oropeza, MSc.). Part of the DFT calculations have been performed by employing the resources of the USFQ's High Performance Computing System. This work employed the Imbabura cluster of Yachay Tech University, which was purchased under contract No.\ 2017-024 (SIE-UITEY-007-2017). The authors thanks the Laser Spectroscopy Laboratory at School of Chemical Sciences, Universidad Central de Venezuela, and Vincent Piscitelli for providing laser fluorescence facilities

Conflicts of Interest: The authors declare no conflict of interest.

Abbreviations

OLEDs	Organic light emission diodes
OFETs	Organic field-effect transistors
TPE	Tetraphenylethane
ACQ	Aggregation-caused quenching
AIE	Aggregation-induced emission
GFP	Green fluorescent proteins
AIEgens	Luminogens with aggregation-induced emission characteristics
DADQs	Diaminodicyanoquinodimethanes
IC	Internal Conversion
ISC	Intersystem-Crossing
TD-DFT	Time dependent – Density Functional Theory
QY	Quantum Yield
S_0	Ground State
S_1	First Excited State
TCNQ	7,7,8,8-Tetracyanoquinodimethane
PTCNQ	7-pyrrolidino-7,8,8-tricyano quinomethane
FTIR	Fourier-transform infrared spectroscopy
DMSO	dimethyl sulfoxide
OD	Optical Density
DFT	Density Functional Theory
PCM	Polarizable continuum Model
ACN	Acetonitrile
LB	Luria Bertani broth base
NICS	Nucleus Independent Chemical Shift

References

1. J. Mei, N. L. C. C. Leung, R. T. K. K. Kwok, J. W. Y. Y. Lam, and B. Z. Tang, "Aggregation-Induced Emission: Together We Shine, United We Soar!," *Chem. Rev.*, vol. 115, no. 21, pp. 11718–11940, Nov. 2015, doi: 10.1021/acs.chemrev.5b00263.

2. M. Zimmer, “GFP: from jellyfish to the Nobel prize and beyond,” *Chem. Soc. Rev.*, vol. 38, no. 10, p. 2823, 2009, doi: 10.1039/b904023d.
3. Y. Hong, J. W. Y. Y. Lam, and B. Z. Tang, “Aggregation-induced emission: phenomenon, mechanism and applications,” *Chem. Commun.*, no. 29, p. 4332, 2009, doi: 10.1039/b904665h.
4. J. Mei, Y. Hong, J. W. Y. Lam, A. Qin, Y. Tang, and B. Z. Tang, “Aggregation-induced emission: The whole is more brilliant than the parts,” *Adv. Mater.*, vol. 26, no. 31, pp. 5429–5479, 2014, doi: 10.1002/adma.201401356.
5. Y. Kagawa *et al.*, “Photo-and electroluminescence for TCNQ-amino adducts,” *Mol. Cryst. Liq. Cryst. Sci. Technol. Sect. A Mol. Cryst. Liq. Cryst.*, vol. 349, no. June 2016, pp. 499–502, 2000, doi: 10.1080/10587250008024971.
6. C. G. Chandaluri, A. Patra, and T. P. Radhakrishnan, “Polyelectrolyte-assisted formation of molecular nanoparticles exhibiting strongly enhanced fluorescence,” *Chem. - A Eur. J.*, vol. 16, no. 29, pp. 8699–8706, 2010, doi: 10.1002/chem.201000502.
7. L.-O. O. Pålsson *et al.*, “Guest–host interactions between dichroic dyes and anisotropic hosts,” *J. Lumin.*, vol. 117, no. 1, pp. 113–122, Mar. 2006, doi: 10.1016/j.jlumin.2005.03.017.
8. C. G. Chandaluri and T. P. Radhakrishnan, “Amorphous-to-crystalline transformation with fluorescence enhancement and switching of molecular nanoparticles fixed in a polymer thin film,” *Angew. Chemie - Int. Ed.*, vol. 51, no. 47, pp. 11849–11852, 2012, doi: 10.1002/anie.201205081.
9. J. B. Birks, *Photophysics of aromatic molecules*. London; new york, 1970.
10. S. W. Thomas, G. D. Joly, and T. M. Swager, “Chemical sensors based on amplifying fluorescent conjugated polymers,” *Chem. Rev.*, vol. 107, no. 4, pp. 1339–1386, 2007, doi: 10.1021/cr0501339.
11. Y. Hong, J. W. Y. Lam, and B. Z. Tang, “Aggregation-induced emission,” *Chem. Soc. Rev.*, vol. 40, no. 11, p. 5361, 2011, doi: 10.1039/c1cs15113d.
12. J. Luo *et al.*, “Aggregation-induced emission of 1-methyl-1,2,3,4,5-pentaphenylsilole,” *Chem. Commun.*, vol. 18, pp. 1740–1741, 2001, doi: 10.1039/b105159h.
13. E. R. Jimenez and H. Rodríguez, “Aggregation-induced emission: a review of promising cyano-functionalized AIEgens,” *J. Mater. Sci.*, vol. 55, no. 4, pp. 1366–1387, 2020, doi: 10.1007/s10853-019-04157-5.
14. S. Jayanty and T. P. Radhakrishnan, “Enhanced Fluorescence of Remote Functionalized Diaminodicyanoquinodimethanes in the Solid State and Fluorescence Switching in a Doped Polymer by Solvent Vapors,” *Chem. - A Eur. J.*, vol. 10, no. 3, pp. 791–797, 2004, doi: 10.1002/chem.200305123.
15. Z. He, C. Ke, and B. Z. Tang, “Journey of Aggregation-Induced Emission Research,” *ACS Omega*, vol. 3, no. 3, pp. 3267–3277, 2018, doi: 10.1021/acsomega.8b00062.
16. H. Fallah-Bagher-Shaidaei, C. S. Wannere, C. Corminboeuf, R. Puchta, and P. v. R. Schleyer, “Which NICS Aromaticity Index for Planar π Rings Is Best?,” *Org. Lett.*, vol. 8, no. 5, pp. 863–866, Mar. 2006, doi: 10.1021/ol0529546.
17. P. Rietsch *et al.*, “Diaminodicyanoquinones: Fluorescent Dyes with High Dipole Moments and Electron-Acceptor Properties,” *Angew. Chemie - Int. Ed.*, vol. 58, no. 24, pp. 8235–8239, 2019, doi: 10.1002/anie.201903204.
18. G. Sezonov, D. Joseleau-Petit, and R. D’Ari, “Escherichia coli Physiology in Luria-Bertani Broth,” *J. Bacteriol.*, vol. 189, no. 23, pp. 8746–8749, Dec. 2007, doi: 10.1128/JB.01368-07.
19. F. M. Ausubel et al., Current Protocols in Molecular Biology: Preface, no. SUPPL. 90. 2010.
20. M. D. Hanwell, D. E. Curtis, D. C. Lonie, T. Vandermeersch, E. Zurek, and G. R. Hutchison, “Avogadro: an open-source molecular builder and visualization tool.” Journal of Cheminformatics 2012, 4:17., [Online]. Available: http://avogadro.cc/.
21. M. J. Frisch, G. W. Trucks, H. B. Schlegel, and G. E. Scuseria, “Gaussian 09.” Wallingford CT, 2016, [Online]. Available: https://gaussian.com.
22. P. Srujana, T. Gera, and T. P. Radhakrishnan, “Fluorescence enhancement in crystals tuned by a molecular torsion angle: A model to analyze structural impact,” *J. Mater. Chem. C*, vol. 4, no. 27, pp. 6510–6515, 2016, doi: 10.1039/c6tc01610c.
23. F. Neese, A. Hansen, and D. G. Liakos, “Efficient and accurate approximations to the local coupled cluster singles doubles method using a truncated pair natural orbital basis,” *J. Chem. Phys.*, vol. 131, no. 6, 2009, doi: 10.1063/1.3173827.
24. N. Scholz *et al.*, “Coumarin-Rhodamine Hybrids—Novel Probes for the Optical Measurement of Viscosity and Polarity,” *J. Fluoresc.*, vol. 27, no. 6, pp. 1949–1956, 2017, doi: 10.1007/s10895-017-2165-4.

25. A. T. Rhys Williams, S. A. Winfield, and J. N. Miller, “Relative fluorescence quantum yields using a Computer-controlled luminescence spectrometer,” *Analyst*, vol. 108, no. 1290, pp. 1067–1071, 1983, doi: 10.1039/an9830801067.